JACS
JOURNAL OF THE AMERICAN CHEMICAL SOCIETY
pubs.acs.org/JACS
Article

Compounded Interplay of Kinetic and Thermodynamic Control over Comonomer Sequences by Lewis Pair Polymerization

Liam T. Reilly,[‖] Michael L. McGraw,[‖] Francesca D. Eckstrom, Ryan W. Clarke, Kevin A. Franklin, Eswara Rao Chokkapu, Luigi Cavallo, Laura Falivene,* and Eugene Y.-X. Chen*

Cite This: https://doi.org/10.1021/jacs.2c10568
Read Online
ACCESS | Metrics & More | Article Recommendations | Supporting Information

ABSTRACT: The design of facile synthetic routes to well-defined block copolymers (BCPs) from direct polymerization of one-pot comonomer mixtures, rather than traditional sequential additions, is both fundamentally and technologically important. Such synthetic methodologies often leverage relative monomer reactivity toward propagating species exclusively and therefore are rather limited in monomer scope and control over copolymer structure. The recently developed compounded sequence control (CSC) by Lewis pair polymerization (LPP) utilizes synergistically both thermodynamic (K_{eq}) and kinetic (k_p) differentiation to precisely control BCP sequences and suppress tapering and misincorporation errors. Here, we present an in-depth study of CSC by LPP, focusing on the complex interplay of the fundamental K_{eq} and k_p parameters, which enable the unique ability of CSC-LPP to precisely control comonomer sequences across a variety of polar vinyl monomer classes. Individual Lewis acid equilibrium and polymerization rate parameters of a range of commercially relevant monomers were experimentally quantified, computationally validated, and rationalized. These values allowed for the judicious design of copolymerizations which probed multiple hypotheses regarding the constructive vs conflicting nature of the relationship between K_{eq} and k_p biases, which arise during CSC-LPP of comonomer mixtures. These relationships were thoroughly explored and directly correlated with resultant copolymer microstructures. Several examples of higher-order BCPs are presented, further demonstrating the potential for materials innovation offered by this methodology.

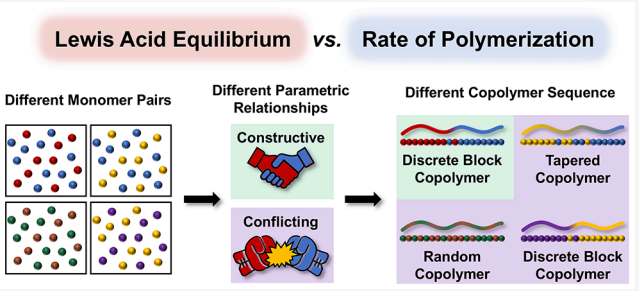

INTRODUCTION

Lewis pair polymerization (LPP),[1−4] which utilizes Lewis acid (LA) and Lewis base (LB) pairs cooperatively to effect monomer activation and polymerization, has continually inspired us over the past 12 years with its ability to solve longstanding polymer synthesis challenges including living/immortal polymerization at room temperature (RT),[5−7] chemoselective polymerization,[8−11] comonomer sequence control and compatibilization,[12,13] and control of polymer topology[8,14−18] and architecture.[19,20] Our recent studies have showcased the compounded sequence control (CSC) methodology, wherein we first disclosed the controlled copolymerization of two highly reactive acrylate isomers, *n*-butyl acrylate (^{n}BA) and *tert*-butyl acrylate (^{t}BA).[12] This initial report demonstrated CSC's ability to achieve highly resolved AB diblock (P^{n}BA-*b*-P^{t}BA) in one pot and one step. Following this proof of concept, we applied CSC to prepare a related ABA triblock (P^{t}BA-*b*-P^{n}BA-*b*-P^{t}BA) in one pot and two steps, which we then transformed into high-performance covalent adaptable networks.[21] We have also reported that ^{n}BA and methyl methacrylate (MMA) are highly compatible for CSC and produce (near) perfect AB sequences (P^{n}BA-*b*-PMMA) with either linear or cyclic block copolymer (BCP) topologies,[22] thus establishing that CSC between different monomer classes is also possible. Most recently, we detailed a mechanistic study on the precision synthesis of cyclic vinyl polymers in which the fundamental mechanisms in LPP that underly CSC were shown to enable spatial and temporal control in the synthesis of cyclic homopolymers and BCPs.[23]

The two-step propagation mechanism of LPP (Figure 1),[4] wherein a free monomer is first coordinated to an equivalent of LA (monomer activation) and then the activated monomer undergoes nucleophilic attack by the active polymeric growing chain (monomer addition), enables CSC and the bulk of the additional polymerization control bolstered by LPP. This two-step propagation presents itself kinetically as a zero-order monomer decay profile characterized by a rate of polymerization = $k_p[LA]_0[LB]_0$. Since the second step (monomer addition) is rate limiting, there is enough time for a prior

Received: October 10, 2022

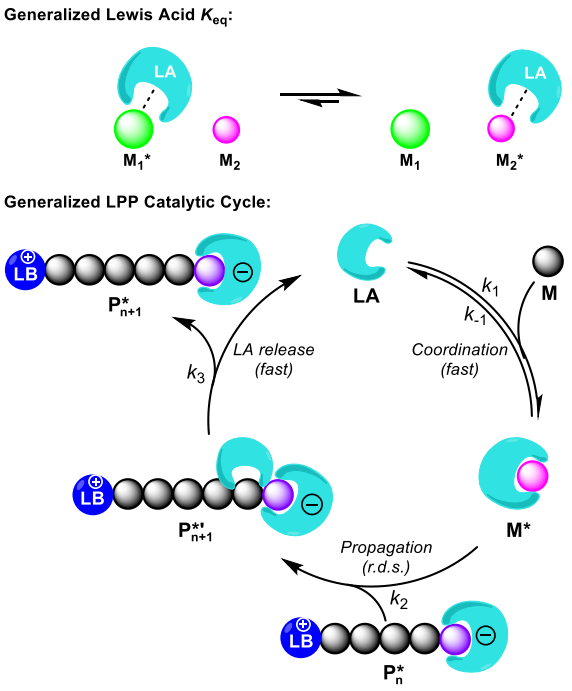

Figure 1. Generalized monomer–LA K_{eq} (top) and LA catalytic propagation cycle (bottom) in LPP.[4]

monomer–LA equilibrium (K_{eq}) to establish itself during the reversible monomer activation step. When only one type of monomer is present, this equilibrium is typically neglected. However, when two (or more) comonomers are present, this monomer–LA equilibrium evolves into a thermodynamic competition for LA coordination (which is at a catalytic concentration) in which one comonomer will have a greater LA-affinity. Thus, a thermodynamic bias for which comonomer is activated by the LA and can enter the rate-determining step (r.d.s.) for monomer enchainment is established (Figure 1).

In any copolymerization of a comonomer mixture, there exists intrinsic kinetic differentiation resulting from the two comonomers' respective rate of polymerization (k_p); i.e., the comonomer with the greater k_p will polymerize with some degree of priority. However, under classical first-order kinetic control, where monomer decay is characterized by $k_p[M]_t[P^*]$ (where $[P^*]$ is the active propagation species concentration), the time-dependent monomer concentration factor, $[M]_t$, will cause the varying polymerization rates of the two comonomers to converge, resulting in an internal domain that is essentially random.[24] We have previously shown that this tapering effect can be substantially suppressed in LPP when the prior equilibrium K_{eq} and the propagation k_p biases compound constructively (Figure 2).[12,22]

We have disclosed two prior examples so far, where K_{eq} and k_p compound constructively using sterically encumbered methyl aluminum-di(2,6-di-*tert*-butyl-4-methyl-phenoxy) (MAD) as the LA and various phosphines as the LB. For example, homopolymerizations of ^{n}BA and ^{t}BA using MAD/PMe_3 reveal a substantial k_p bias, where $k_p^{(nBA)}/k_p^{(tBA)}$ equals ~30 and the K_{eq} of the 1:1:1 (^{n}BA/^{t}BA/MAD) mixture was measured to be ~16 at RT favoring the [^{n}BA·MAD] adduct. Thus, both k_p and K_{eq} parameters are biased toward ^{n}BA and are therefore synergistically constructive. Under such circumstances, the kinetic tapering effect is diminished—as the monomer that is predominantly LA-activated also undergoes

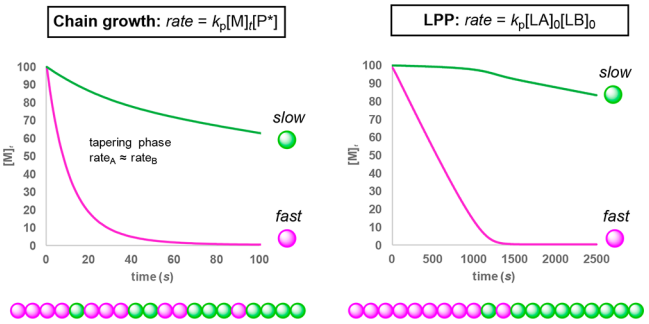

Figure 2. Illustrative comparison of the resulting BCP microstructure of typical chain-growth polymerization and LPP, highlighting the suppression of the kinetic tapering phase achieved through CSC-LPP.[4]

the addition step more quickly. In our work, we have also encountered scenarios in which k_p and K_{eq} parameters conflict and bias opposite monomers. We initially hypothesized that such a relationship would amplify tapering—as one monomer is predominantly LA-activated but slower to undergo the addition step, while the alternate comonomer is less frequently LA-activated but more readily incorporated when it is. In probing this hypothesis, we instead unearthed unique insight into the fundamental k_p and K_{eq} interplay that governs the degree of comonomer sequence control exhibited by this distinctive methodology. Accordingly, herein we report our systematic, combined experimental and computational investigation of the complex relationship between the thermodynamic competition for LA-coordination (K_{eq}) and relative rates of polymerization (k_p) for a variety of commercially relevant polar vinyl monomer classes (acrylates, methacrylates, and acrylamides, as well as bio-renewable sorbates and α-methylene lactones) evaluated for their potential to form discrete BCPs in one pot and one step from premixed monomer feeds. Additionally, we offer several examples of how these fundamental insights can be applied for innovation in creating novel polymers, including strategies for the facile (one pot and one step) preparation of ABC tri-BCPs, ABA/ABCBA tri/penta-BCPs for thermoplastic elastomer (TPE) applications, and a unique crosslinkable di-BCP with modular thermal properties.

■ RESULTS AND DISCUSSION

We began our investigation by selecting a suite of representative monomers across a range of polar vinyl monomer classes (Figure 3) including acrylates [^{n}BA, ^{t}BA, MA (methyl acrylate), AIA (allyl acrylate)], MMA, *N*,*N*-dimethyl acrylamide (DMAA), and bio-based α-methylene-γ-methyl-γ-butyrolactone (MMBL) and ethyl sorbate (ES). These monomer classes were selected for their commercial relevance and relative structural differences that we hypothesized should give rise to a wide variety of K_{eq} and k_p values, which would enable the analysis of the fundamental relationship between these parameters across the extremes of constructive and conflicting scenarios. Despite the ever expanding variety of LPs made available by recent work in organocatalysis[25−31] and main-group FLP chemistry,[32−35] we determined maintaining a consistent LP across this study was most appropriate; in the interest of limiting variables and maintaining internal consistency for relative comparisons, MAD was the selected LA examined, while the LB was usually

https://doi.org/10.1021/jacs.2c10568
J. Am. Chem. Soc. XXXX, XXX, XXX−XXX

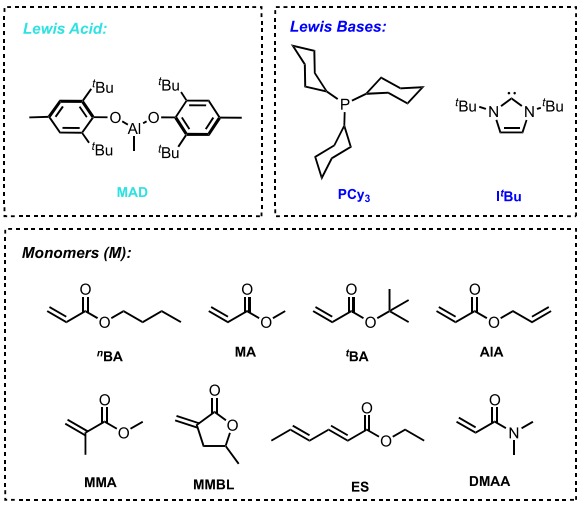

Figure 3. Scope of monomers and Lewis pairs (LPs) employed throughout this study.

tricyclohexylphosphine (PCy_3), except for a few specific cases where the *N*-heterocyclic carbene 1,3-di-*tert*-butylimidazolin-2-ylidene (I^tBu) was more appropriate (see Table 1 for details).

Systematic Evaluation of K_{eq} and k_p Parameters. We first approximated the LA-affinity of each candidate comonomer (M) by measuring the equilibrium constant (K_{eq}) in a reaction involving [M]/[^{n}BA]/[MAD] = [0.027]:[0.027]:[0.027] M in toluene-d_8. Provided the extent of our experience with ^{n}BA in two prior studies,[12,22] we measured LA-affinities of other monomers against that of ^{n}BA. This approach ensured a standard to which each new monomer of interest could be compared, such that evaluating every iterative monomer combination was not necessary. We generally assumed that the transitive property was applied (e.g., MMBL has a greater MAD-affinity than ^{n}BA and will therefore have a greater MAD-affinity than MMA, which has a lower MAD-affinity than ^{n}BA) and have never observed an exception. In this experiment, both ^{n}BA and comonomer M compete for coordination to the single molar equivalence of MAD. The ^{n}BA- and M-coordinated structures have unique ^{1}H-NMR signals, the most convenient of which (for analysis) being the MAD Al-CH_3 signal, typically observed without competitive peak overlap between 0 and −1 ppm depending on the chemical environment. Integration and evaluation of both M·MAD and ^{n}BA·MAD peaks can be used to formulate a K_{eq} value based on eq 1, where [^{n}BA·MAD] is directly measured and [M] is logically inferred to be equal to [^{n}BA·MAD]. Similarly, [M·MAD] is directly measured, and [^{n}BA] is inferred to be equal to [M·MAD].

$$K_{eq} = \frac{[M][^nBA{\cdot}MAD]}{[M{\cdot}MAD][^nBA]} \quad (1)$$

The equilibrium exchange between the two coordinated structures is often too rapid to be resolved by ^{1}H-NMR at RT. Therefore, low-temperature ^{1}H-NMR is employed to slow this exchange and fully resolve both chemical environments. In our previous study, we measured the K_{eq} of ^{n}BA vs ^{t}BA at several different temperatures between −20 and −60 °C to generate a van't Hoff plot, which was used to extrapolate the K_{eq} at RT.[12] We found that this level of analysis was only possible because of the structural similarity of ^{n}BA and ^{t}BA, which gave K_{eq} values closer to 1 (20 at −20 °C). However, when two structurally disparate monomers are measured by the same method, the K_{eq} becomes more extreme, which implicates signal-to-noise ratio errors when integrating the ^{1}H-NMR signal of the minor environment. As a result, our attempts to extrapolate RT K_{eq} values via the generated van't Hoff plots gave nonlinear trends. We, therefore, opted to report the K_{eq} values that we could measure at −20 °C to convey the qualitative degree and direction of the LA-affinity bias for each monomer pair. In all cases, we found that the K_{eq} bias moves closer to 1 with increasing temperature (i.e., higher temperatures are less selective for sequencing). Additionally, the exothermicity of these polymerizations causes the temperature to change during the course of the reaction so that unless the temperature is tightly controlled, instantaneous K_{eq} values are time dependent and thus futile to consider quantitatively. The results of our investigation can be seen in Figure 4, while the

Table 1. Selected Results of CSC Copolymerizations[a]

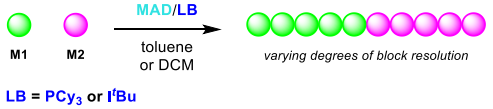

run	M_1	M_2	[M]	M_1/M_2/LA/LB	M_n[c] (kDa)	$Đ$[c]	T_g (°C)
1	^{n}BA	^{t}BA	1.20	1000:1000:10:1	199	1.08	−39.0, 47.2
2	^{n}BA	MMA	1.20	500:500:10:1	126	1.06	−44.2, 127
3	AlA	MMA	1.20	500:500:10:1	125	1.01	−29.9, 130
4	^{t}BA	MMA	1.20	200:200:2:1	86.1	1.09	49.0, 127
5	^{n}BA	MMBL	2.40	250:250:5:1	62.3	1.18	101
6[b]	^{n}BA	ES	1.20	200:200:4:1	58.0	1.55	−43.0, −1.70
7	^{t}BA	MMBL	2.40	100:100:2:1	33.7	1.10	42.6, 202
8	MMBL	MMA	2.40	100:100:2:1	27.4	1.04	216, 125
9[b]	ES	MMA	1.80	200:200:2:1	35.1	1.17	38.5
10[b]	MMBL	ES	1.20	250:250:5:1	90.1	1.19	213, 2.30

[a]Conditions: 20 °C; M1, M2, and MAD were premixed in toluene (or DCM, for MMBL runs) at appropriate concentrations according to 0.50 mL of M1, PCy_3 was injected as 0.20 mL of a stock solution prepared in toluene. [b]I^tBu was used instead of PCy_3 (toluene is still used for the stock solution, even for MMBL runs, due to the instability of I^tBu in DCM). [c]Weight-average molecular weight (M_w), number-average molecular weight (M_n), and dispersity ($Đ = M_w/M_n$) determined by gel-permeation chromatography coupled with a multi-angle light scattering detector for absolute molecular weights.

https://doi.org/10.1021/jacs.2c10568
J. Am. Chem. Soc. XXXX, XXX, XXX−XXX

NMR spectra from which the values are derived are Figures S3–S6.

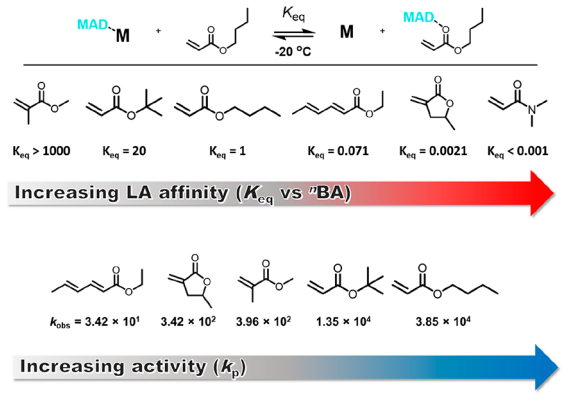

Figure 4. LA-affinities (top) of representative monomers from various classes probed by measuring the K_{eq} for MAD coordination vs ^{n}BA and homopolymerization k_p measurements (bottom) for representative monomers in MAD-catalyzed LPPs, where units of k_p are $[M]\cdot s^{-1}[MAD]_t[LB]_0$.

Our benchmark report included the K_{eq} study of ^{n}BA vs ^{t}BA, which have similar molecular electronics but differ by the degree of steric congestion surrounding the ester group. Our work since then suggests that electronic differences between comonomers lead to even more extreme K_{eq} biases, which is ideal for CSC copolymerizations. For example, the α-methyl substitution found on methacrylates (which is absent for acrylates) strongly deactivates the methacrylate carbonyl (lowering its basicity) such that acrylates completely dominate methacrylates in terms of LA-affinity. Conversely, β-substitution increases the basicity of the carbonyl giving crotonates and sorbates greater LA-affinity than acrylates and methacrylates. This increased affinity can be rationalized by considering that β-substituted monomers have a resonance form containing a secondary carbocation where acrylates and methacrylates contain a less stable primary carbocation. Similarly, sorbates have a greater LA-affinity than crotonates due to the additional resonance form afforded by a second conjugated alkene. Intriguingly, α-methylene lactone MMBL exhibits an extremely high LA-affinity, as the molecule is locked in a planar *S-cis* configuration ideal for LA-coordination and the ester is oriented away from the carbonyl and coordinated LA, which minimizes steric tension. Lastly, acrylamide DMAA completely dominates every other monomer class in competition for LA coordination, unsurprisingly, due to electron donation from the amide nitrogen. However, copolymerizations between DMAA and acrylates resulted in homopolymer PDMAA with no conversion of the acrylate, because the PDMAA carbonyls have such great LA affinity that they completely sequester the LA and therefore exclude the acrylate comonomer. While interesting, this practical incompatibility led us to exclude acrylamides from further evaluation.

The second part of our investigation involved the determination of comparable activity values (k_p) for each monomer by in situ tracking of monomer consumption vs time. There are a few considerations important to this experimental design. First, due to the extreme differences in activity (nearly 5 orders of magnitude between ^{n}BA and ES), LP concentration was varied between monomers to extend or reduce the time scale of each polymerization such that the [M] vs time could be reliably tracked. Thus, the polymerization rate, measured by calculating the slope ($[M]\cdot s^{-1}$) of a [M] vs time plot, was normalized by dividing the measured $[M]\cdot s^{-1}$ by $[LA]_t[LB]_0$ so that the units (ü) for normalized activity become $[M]\cdot s^{-1}\cdot[LA]_t^{-1}\cdot[LB]_0^{-1}$, where $[LA]_t$ is the $[LA]_0$ after subtracting the LA equivalent that reacts with the monomer and LB during the initiation step. This normalization is meant to mimic the rate law, which is generally accepted to follow $k_p[LA]_t[LB]_0$. Second, since monomer activity within LPP is sensitive to LP structure, MAD/PCy_3 was used consistently, when possible, to ensure the generated rate data would be valid for comparative purposes. As previously mentioned, there were exceptions for some monomers within the scope that are not efficiently initiated using MAD/PCy_3, most likely due to insufficient nucleophilicity of the sterically hindered PCy_3. In these cases, we prepared a discrete initiating species by reacting an equivalent of ^{n}BA with one equivalent of MAD/PCy_3 (1,1:1) to generate the corresponding phosphonium enolaluminate zwitterion. This so-called active ^{n}BA onemer was capable of rapid and efficient initiation and was employed for the polymerizations of MMBL, MMA, and ES. Importantly, this approach maintained the identical cationic PCy_3^+ at the polymer α-terminus. It was crucial to preserve the identity of the LB for these polymerizations examining k_p, as the cationic α-terminus is electrostatically paired to the anionic ω-terminus throughout polymerization and therefore mediates the transition states of propagation.[4,36] Thus, the LB structure remains relevant well after initiation is complete. However, once we established rate data for these monomers, we opted to use I^{t}Bu for the remainder of the study in place of the ^{n}BA onemer as it is equally efficient and much more convenient to work with. Importantly, we verified that the general trend for reactivity and sequencing held true with this swap of LB ($k_p^{MMA} > k_p^{MMBL} > k_p^{ES}$). Lastly, toluene was the solvent used for all the kinetic evaluations with the exception of the MMBL run, for which dichloromethane (DCM) was used due to solubility constraints of the polymer PMMBL (which precipitates in toluene midway through the reaction).

With these considerations in mind, we found the activities to be ordered as follows: ES was the slowest among all monomers with a k_{obs} of 3.42×10^1 ü (ü = $[M]\cdot s^{-1}\cdot[MAD]_t^{-1}\cdot[LB]_0^{-1}$). Next, MMBL showed a 10-fold rate increase compared to ES, with a k_{obs} of 3.42×10^2 ü. MMA exhibited a marginally greater k_{obs} of 3.96×10^2 ü. This trend is unsurprising as MMBL, being a cyclic analogue of MMA, is structurally similar to methacrylates containing alkenyl methylene as well as substitution at the α-carbon. Lastly, acrylates possessed by far the greatest polymerization activity, as expected.

To gain a general understanding of the effect of steric hindrance within one monomer class, we compared ^{n}BA with ^{t}BA. In our previous report,[12] using PMe_3 as opposed to PCy_3, we observed an approximate 30-fold difference in activity between ^{n}BA and ^{t}BA. However, when the bulkier PCy_3 is employed, ^{n}BA activity is diminished, while ^{t}BA activity remains relatively unaffected. The resulting difference in activity is almost threefold with ^{n}BA giving a k_{obs} of 3.85×10^4 ü and ^{t}BA giving a k_{obs} of 1.35×10^4 ü. This observation shows that the LB can be an effective handle for optimizing the degree of comonomer sequencing and block resolution and should be considered as such for future optimizations.

Effects of Differing K_{eq}/k_p Relationships on Block Resolution in One-Pot BCPs. Following the quantification of the fundamental K_{eq} and k_p parameters and confirming that

https://doi.org/10.1021/jacs.2c10568
J. Am. Chem. Soc. XXXX, XXX, XXX−XXX

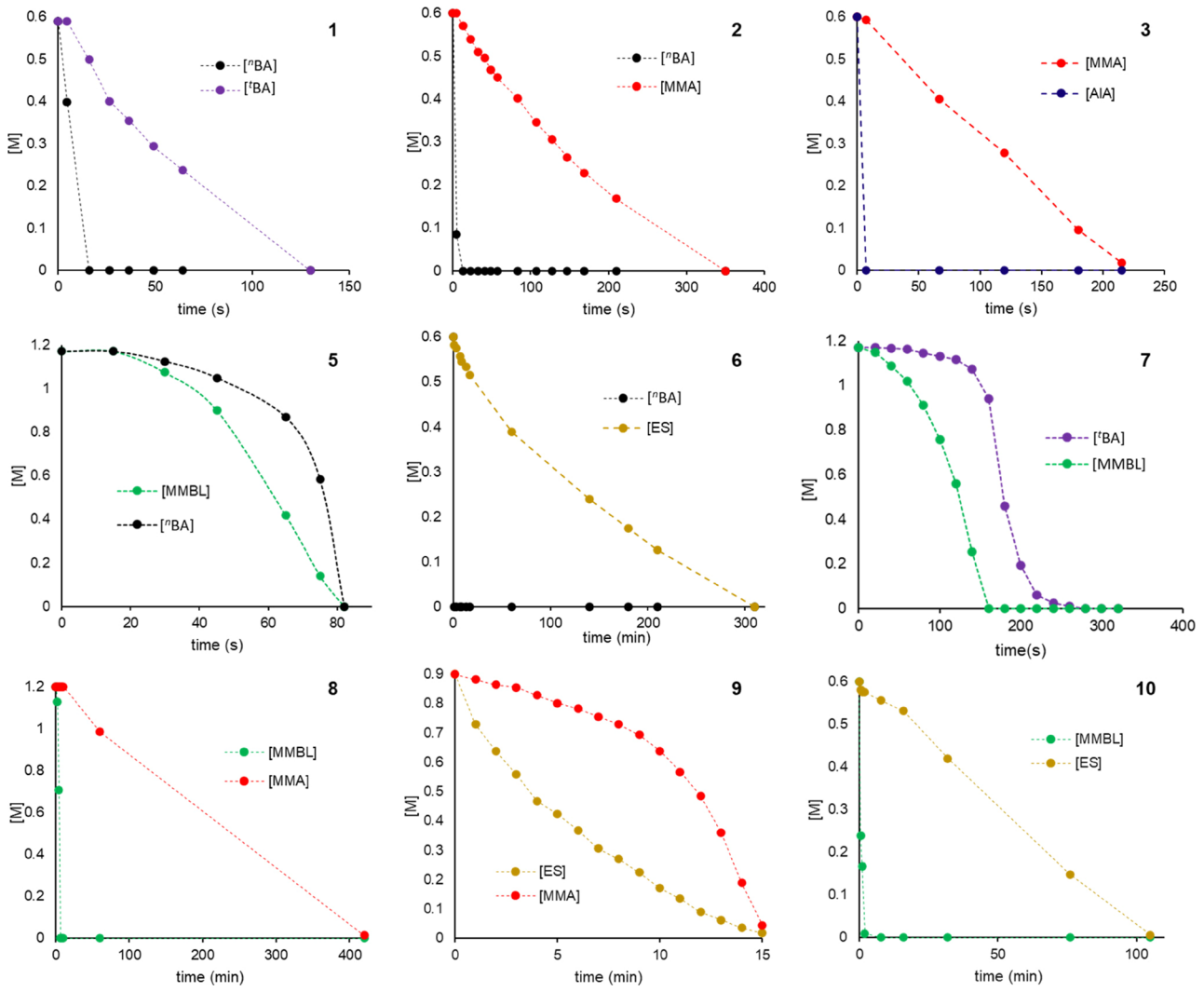

Figure 5. Kinetic profiles of selected copolymerizations revealing differing patterns of comonomer incorporation over time based on the degree of comonomer sequencing. Numbers **1**−**3** and **5**−**10** represent run numbers reported in Table 1.

indeed our selection of monomers provided a satisfactory range of potential relationships, we judiciously designed copolymerizations to answer several questions regarding the nature of the relationship between the thermodynamics of the monomer−LA equilibrium and the kinetics of propagation.

To determine the degree of comonomer sequencing and the resulting polymer microstructure, we employed several modes of analysis. First, differential scanning calorimetry (DSC) was utilized to observe the thermal transitions of the resultant polymers. Importantly, the homopolymers of each monomer in our selected scope have non-overlapping glass transition temperature (T_g) values. This feature enables us to discern the degree of comonomer sequencing and resolution of the resultant blocks of each copolymer via analysis of the number of T_g's and the shift of these transitions relative to that of the respective homopolymers. More explicitly, the presence of two T_g's in the copolymer DSC trace represents the aggregation of two unique domains, which is indicative of a self-assembled blocky microstructure. Alternatively, the presence of one composite T_g indicates a low degree or complete lack of comonomer sequencing and only one polymeric domain. ^{13}C-NMR was additionally employed, as the resolution and patterning of the ester carbonyl carbon peak in the spectra of these polymers have proven useful for differentiating random and block microstructures. Lastly, and most directly, in situ kinetic tracking of monomer consumption (incorporation) over the course of polymerization proved most useful. ^{1}H-NMR of quenched aliquots of the polymerization reaction over time revealed either simultaneous comonomer incorporation (lack of sequencing) or completely staggered comonomer incorporation (perfect sequencing).

For experimental consistency across these copolymerizations, we used toluene as the solvent in all cases except for the runs involving MMBL, again owing to the solubility constraints of PMMBL. Additionally, the initial monomer concentrations and initial MAD concentrations were specifically chosen for each experiment on a case-by-case basis to adjust reaction rates so that each reaction could be tracked within a reasonable timeframe. These concentration parameters should in theory have no effect on comonomer sequencing or block resolution.

Constructive CSC of Sterically Disparate Comonomers. Within a given monomer class, steric considerations appear most relevant for sequencing compatibility, as electronic differences between related monomers are quite minor. The isomeric acrylate pair of ^{n}BA and ^{t}BA, which possess a constructive k_p and K_{eq} bias in favor of the less hindered ^{n}BA,

https://doi.org/10.1021/jacs.2c10568
J. Am. Chem. Soc. XXXX, XXX, XXX−XXX

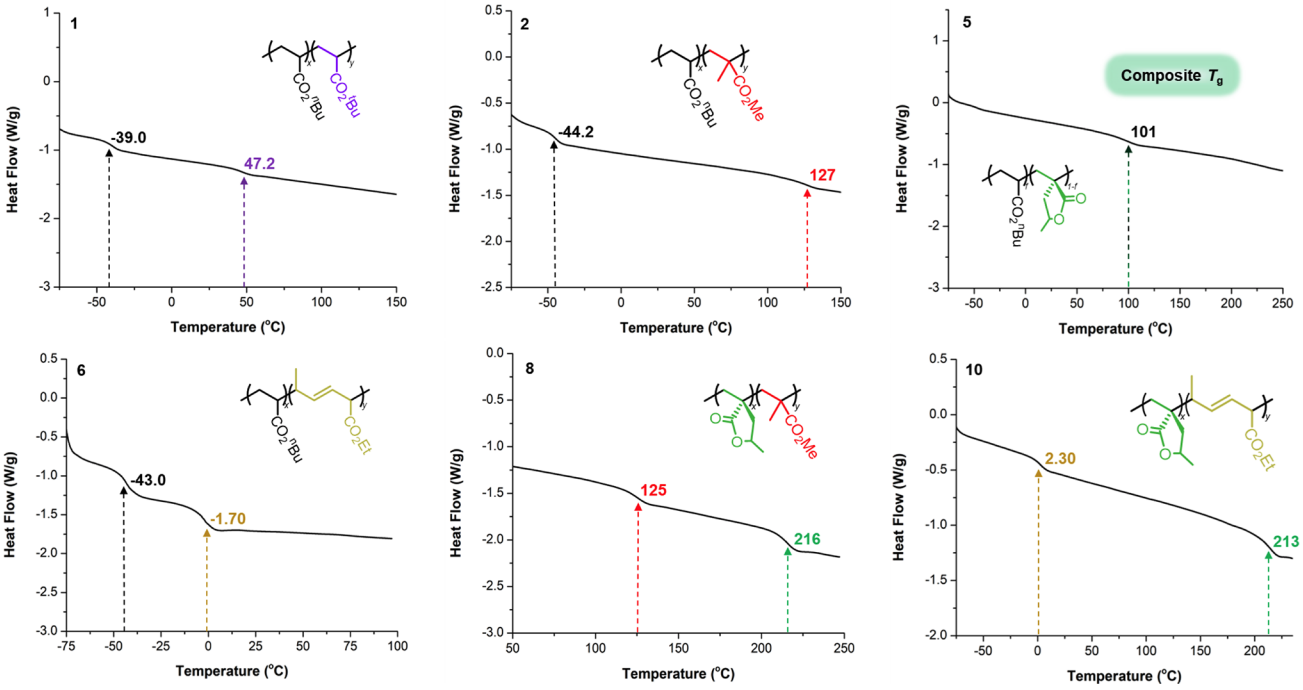

Figure 6. DSC curves of selected copolymers obtained from copolymerizations (runs 1, 2, 5, 6, 8, and 10 of Table 1), revealing differing patterns of phase transitions as reflected by glass transitions based on the degree of comonomer sequencing. Numbers **1**, **2**, **5**, **6**, **8**, and **10** represent run numbers reported in Table 1.

demonstrates the starkest contrast in steric hindrance between the primary and tertiary alkyl ester groups. Despite still imperfect block resolution, the DSC trace contained two T_g's at −39.0 and 47.2 °C for the ^{n}BA and ^{t}BA domains, respectively, indicative of a blocky structure. This experiment further demonstrates the importance of the compounding thermodynamic bias introduced through the use of the sterically bulky and differentiating LA MAD, as the same polymerization performed using a less sterically significant and non-differentiating LA (representative of classical anionic polymerization) resulted in a random copolymer with a single T_g.[12] We also evaluated ^{n}BA with many secondary esters such as isobornyl acrylate, phenyl acrylate, and cyclohexyl acrylate, but observed negligible sequencing as judged by the presence of only one composite T_g on the DSC curves. With the MAD/PCy_3 LP, we did not observe significant sequencing behavior between any additional acrylate monomers apart from ^{n}BA/^{t}BA (Table 1, run 1); however, this does not preclude the possibility of achieving enhanced sequencing between such monomers within the same class if a more optimal LP is employed.

Constructive CSC of Electronically Disparate Comonomers. The acrylate/methacrylate pairing is ideal for CSC since there are massive biases for both thermodynamic K_{eq} and kinetic k_p parameters that constructively compound to give nearly perfect block resolution. This CSC was already demonstrated in our previous report, with ^{n}BA/MMA and ^{n}BA/allyl methacrylate pairs.[22] In this study, we included a select few acrylates and tested them against MMA with a more thorough examination by tracking monomer consumption over time. Unsurprisingly, the ^{n}BA/MMA (Table 1, run 2) sequence is nearly perfect as judged by the kinetic profile (Figure 5) and the DSC trace (Figure 6). We also selected AlA as a second candidate to showcase the chemoselective nature of this LPP and demonstrate the opportunity for post-functionalization following a sequence-controlled LPP. The AlA/MMA reaction (Table 1, run 3) sequenced nearly perfectly. Impressively, the aliquot of the reaction taken for the kinetic profile (Figure 5, **3**) at 7 s shows quantitative consumption of AlA while ∼99% of the original MMA remained. This remarkable block resolution is maintained even when the more sterically hindered ^{t}BA is polymerized in the presence of MMA as judged by the presence of two T_g's (Figure 6). Thus, as a general rule, we can expect that any acrylate will express a high degree of sequence control when paired with any methacrylate, as long as both monomers are compatible with LPP.

Conflicting CSC of Comonomers with Highly Differing k_p and LA-Affinities. With both previously reported CSC copolymerizations consisting of comonomers with significantly constructive K_{eq}/k_p relationships, we elected to examine the sequencing of acrylates with MMBL, a representative monomer from an emerging class of high T_g biorenewable materials.[37−39] Each acrylate within our monomer scope possessed substantially greater polymerization activity but much lower LA-affinity than MMBL, and therefore, this pairing served as an ideal starting point for the investigation into the more nuanced CSC comonomer relationships.

Beginning with ^{n}BA/MMBL, which maximized the conflict between K_{eq} and k_p biases, and continuing with MA/MMBL and ^{t}BA/MMBL, we expected to produce a series of random or tapered copolymers highlighting the importance of the constructive relationship between the thermodynamic K_{eq} and kinetic k_p biases required for discrete comonomer sequencing. Indeed, when ^{n}BA and MMBL were polymerized together, the resulting polymer was essentially random with a single composite T_g (Figure 6, **5**) of 101 °C, which is satisfyingly between the two homopolymer T_g's of −45.0 and 216 °C, respectively. The kinetic profile (Figure 5, **5**) beautifully illustrates the competitive nature between the two

https://doi.org/10.1021/jacs.2c10568
J. Am. Chem. Soc. XXXX, XXX, XXX−XXX

comonomers, and therefore the thermodynamics of LA-activation and kinetics of polymerization. MMBL is incorporated at a slightly greater rate initially, however, after a significant amount of the MMBL is depleted, the ^{n}BA is then activated by the progressively available MAD, and thereby the ^{n}BA rate of incorporation dramatically increases as the reaction progresses. Note that since PCy_3 must initiate on an LA-activated equivalent of ^{n}BA and cannot initiate on LA-activated MMBL, an induction period is observed; the initiation process is slow and concludes at the point when the [MMBL] curve becomes linear. The MMBL/MA CSC gives a comparable profile.

To our surprise, the CSC of ^{t}BA/MMBL revealed a most interesting phenomenon. The decreased LA-affinity of ^{t}BA (compared to ^{n}BA and MA, Figure 4) further increases the thermodynamic bias for MMBL to the point that the kinetic bias for the acrylic ^{t}BA is overridden; the copolymerization generated a substantial degree of comonomer sequencing and block resolution. While they do not sequence perfectly, there is enough resolution to produce two T_g's on the DSC, suggesting sufficient block character for domain aggregation. We find this example particularly important, as our previously reported examples of sequencing between ^{n}BA/^{t}BA and ^{n}BA/MMA have both been parametrically constructive examples where one might be tempted to think that the great difference in k_p of ^{n}BA/^{t}BA or ^{n}BA/MMA was the sole reason for the sequencing effect and that the K_{eq} bias was ancillary or unimportant. This parametrically conflicting example of MMBL/^{t}BA demonstrates the importance of the K_{eq} bias, as ^{t}BA is ∼40 times more active than MMBL, yet MMBL still takes greater priority and sequences first due to its highly pronounced LA-affinity.

Conflicting CSC of Comonomers with Minimally Differing k_p and Greatly Differing LA-Affinities. This observation of comonomer sequencing within a parametrically conflicting CSC (^{t}BA/MMBL) deepened our understanding of the interplay between thermodynamics and kinetics at the core of the CSC mechanism. To further evaluate the intriguing possibility of achieving comonomer sequencing between conflicting monomer pairings, we examined the copolymerization of the MMBL/MMA pair. Within our monomer scope, this combination minimized (but maintained) a conflicting kinetic bias, in favor of MMA, while exaggerating the thermodynamic bias in favor of MMBL (2 order of magnitude decrease in kinetic bias, 3 order of magnitude increase in thermodynamic bias, compared to MMBL/acrylate pairs, Figure 4). This exaggerated K_{eq} and minimally conflicting k_p results in a copolymerization in which MMBL dominates and MMA is completely excluded until MMBL is depleted (Figure 5, **8**). These two monomers sequence seemingly perfectly. However, there is an inconvenience in that the PMMBL carbonyls retain considerable LA-affinity, which competitively disrupts the MMA activation even after full MMBL depletion. Consequently, these polymerizations require extended time periods to reach full conversion of MMA. Both T_g's can be observed on the DSC (Figure 6, **8**). This run further confirmed the significance of the K_{eq} bias and the ability of the thermodynamics of the LA equilibrium to exclusively select for one comonomer's incorporation in the face of a kinetic disadvantage—this observation inspires the possibility that previously considered CSC-incompatible monomer pairings might be sequenced through optimization of LA structure for the rebalancing of comonomer K_{eq}.

The delicacy of the balance between the thermodynamic equilibrium and kinetic rate differences that enable CSC is revealed by evaluation of the ES/MMA pairing, which possess a parametrically similar relationship to MMBL/MMA, yet surprisingly different polymerization behavior. Like MMBL, ES is strongly favored by the thermodynamics of the LA K_{eq} and is at a kinetic disadvantage to the methacrylate. However, ES has a lesser LA-affinity than MMBL (by ∼34 times) and is also ∼10 times less active for polymerization. In comparison to other monomer pairings, the magnitude of this difference is quite insignificant. Nonetheless, this shift was enough to allow for competitive MMA incorporation throughout the copolymerization of the ES/MMA mixture, observed as a unique tapering profile in which the decay curves show a concave/convex pattern (Figure 5, **9**). ES exhibits a slightly greater priority early in the reaction while the MMA rate increases over time. This particular example is an ideal profile for conflicting CSC parameters where the interplay is well represented—the thermodynamic advantage is expressed early as the ES outcompetes MMA for LA-activation, but as the concentration of ES drops, the kinetically advantaged MMA rapidly increases its rate of incorporation. Once ES reaches a concentration at which the abundance of MMA allows for a more competitive instantaneous K_{eq}, the MMA actually outcompetes ES for incorporation.

Conflicting CSC of Comonomers with Greatly Differing k_p and Minimally Differing LA-Affinities. Curious as to whether a significant enough kinetic bias could similarly outright override a conflicting thermodynamic bias, we examined the copolymerization of ^{n}BA/ES. This pairing is ideal, as it exemplifies the most extreme kinetic bias available within our monomer scope (^{n}BA is ∼1100 times more active than ES) while maintaining a minimized yet respectable conflicting thermodynamic bias (K_{eq} = 0.071, favoring ES by ∼14:1). Excitingly, the k_p bias of ^{n}BA overwhelms the marginal K_{eq} advantage expressed by ES. The copolymerization resulted in nearly perfect comonomer sequencing (Figure 5, **6**) and two T_g's are observed by DSC (Figure 6, **6**). This result demonstrates that highly disparate rates of polymerization can indeed serve as a selective kinetic barrier and enable comonomer sequencing in light of a conflicting thermodynamic equilibrium. This again reshaped our preconceptions regarding requirements for CSC-compatible comonomers and further implies that reaction conditions that disproportionately alter rates of polymerization between monomer classes might be used as a handle to modulate the degree of sequence control by exaggerating or minimizing k_p bias within a monomer pair.

Constructive CSC of Comonomers with Minimally Differing k_p and LA-Affinities. Having examined the extremes of conflicting and constructive CSC relationships, several conclusions were apparent: strongly constructive relationships produce near perfect comonomer sequencing, as do relationships in which the bias of one parameter dominates that of the other. Tapered and random copolymers are produced in more nuanced conflicting relationships in which the balance between biasing parameters is not as extreme. However, we had yet to explore the lower limit of constructive relationships across monomer classes, and it was unclear whether some threshold of compounding parameters was required for the formation of discrete BCPs of a minimally constructive pairing of comonomers.

https://doi.org/10.1021/jacs.2c10568
J. Am. Chem. Soc. XXXX, XXX, XXX−XXX

As such, the MMBL/ES pair was evaluated. These monomers neighbor one another in both LA-affinity and rate of polymerization and thus provide the least compounding of constructive CSC parameters possible within our scope (across monomer classes). As MMBL is favored in both k_p and K_{eq} terms, satisfyingly, the CSC of MMBL/ES shows practically complete conversion of MMBL prior to incorporation of ES, resulting in near ideal block resolution (Figure 5, **10**). The DSC shows two T_g's at 213 (PMMBL) and 2.30 °C (PES) corresponding to the two highly resolved homogenous domains (Figure 6, **10**). Beyond confirming that the lower end of constructive relationships still produces nearly perfect comonomer sequence control, we found this pair especially interesting since they are both bio-sourced monomers with highly disparate thermal and mechanical properties.

Theoretical Basis of CSC in LPP. To further rationalize the CSC-LPP results for the considered monomers, density functional theory (DFT) calculations were carried out. At first, the thermodynamics for the formation of the M-MAD adduct were calculated by computing the ΔG for the complexation reaction (Table 2).

Table 2. Free Energies (Toluene) for M-MAD Adduct Formation and Electronic Charges Calculated on the Carbonyl Oxygen in the Free M

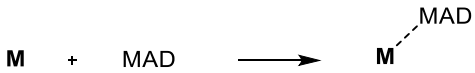

M	ΔG (kcal/mol)	charge on carbonyl O (e)
MMA	−4.8	−0.198
^{t}BA	−7.9	−0.205
^{n}BA	−8.3	−0.203
ES	−10.0	−0.214
MMBL	−11.5	−0.155
DMMA	−12.1	−0.237

As can be seen from the data reported in Table 2, the calculated ΔG values well reproduce the trend in the measured K_{eq} (Figure 4) spanning from an energy gain of only 5.0 kcal/mol for the formation of MMA/MAD adduct with this monomer showing the lowest affinity toward the LA, to an energy gain of almost 12 kcal/mol in case of DMMA. A clear trend emerges from comparing the charges on the carbonyl oxygen calculated on the free monomer: the more the oxygen is electron rich the greater is the affinity toward the LA, going from a relatively electron poor oxygen in MMA with a charge of −0.198e to a quite electron rich oxygen in DMMA with a charge of −0.237e (Table 2).

The only exception among the considered monomers is MMBL that shows a good LA-affinity despite a quite low electron density on the carbonyl oxygen atom. The peculiarity of this monomer, the only cyclic one in the group, is due to the steric contribution winning over the electronic one. Specifically, comparing the geometry of the MMBL/MAD adduct with the one of its corresponding linear acyclic monomer MMA reveals that the low steric requirement of MMBL makes the difference and affects positively the stability of the LA adduct (Figure 7). In the adduct with the acyclic monomers the encumbered substituents lying on the Al center end up crashing with both the "head" and the "tail" of the monomer with several short carbon−carbon distances that affect the stability of the adduct. Instead, the cyclic conformation of

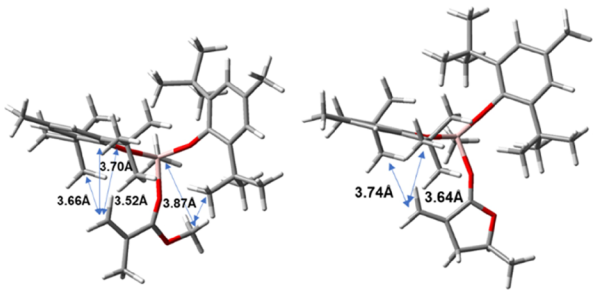

Figure 7. Optimized geometries of the MAD adduct with MMA (left) and MMBL (right).

MMBL minimizes these unfavorable interactions, as the ester tail is oriented away from the MAD.

Moving to the relative activity of polymerization, we have found the stability of the zwitterionic intermediate formed by addition of the LB to the M-MAD adduct well correlating with the observed k_p (Table 3). As the formation of the zwitterion

Table 3. Free Energies (kcal/mol in Toluene) for the Formation of the LB-M-MAD Zwitterionic Adduct (LB = I^{t}Bu)

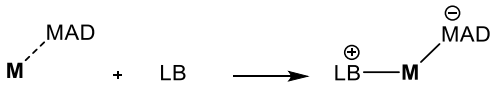

M		ΔG (kcal/mol)
ES	0.0	−4.8
MMBL	0.0	−16.4
MMA	0.0	−16.5
^{t}BA	0.0	−19.3
^{n}BA	0.0	−19.9

completes the initiation step, it is the essential step leading to the propagation cycle of the LPP. The free energy data reported in Table 3 show that steric and electronic properties of the monomer affect to the same extent both the reactivity of the monomer−LA adduct with the LB and the reactivity of the resulting zwitterionic species during the chain growth. To explain the observed differences among the monomers and potentially provide a rational guide for any future experimental design, we looked further for molecular descriptors able to capture these behaviors. As for the steric analysis, we calculated the $\%V_{Bur}$[40] of the monomer around the conjugated β-carbon (Table 4).

The two monomers with a k_p of 10^4 order and a stability of the zwitterionic intermediate of almost −20 kcal/mol, ^{n}BA and ^{t}BA, have the lowest $\%V_{Bur}$ of around 35. Next, the two methacrylate monomers with a k_p of 10^2 order, MMA and MMBL, show an increased $\%V_{Bur}$ of around 40. Finally, ES

Table 4. $\%V_{Bur}$ Calculated on the Free Monomer and Electronic Charges (e) on Conjugated β-Carbon Calculated on the M-MAD Adduct

M	$\%V_{Bur}$	charge on conjugated β-carbon
ES	42.7	−0.101
MMBL	39.8	−0.0183
MMA	40.0	−0.0183
^{t}BA	35.2	0.00754
^{n}BA	35.1	0.00638

https://doi.org/10.1021/jacs.2c10568
J. Am. Chem. Soc. XXXX, XXX, XXX−XXX

with a k_p of 10^1 and a zwitterionic intermediate being much less stable than the others has the greatest hindrance around the β-carbon, with a $\%V_{Bur}$ of almost 43.

The electronic effects are reflected by the charges calculated on the β-carbon in the M-MAD adduct reported in Table 4. In detail, the two acrylate monomers carry the lowest electronic density on the β-carbon, thus the highest electrophilicity. As a consequence, they exhibit the highest reactivity toward the LB in the initiation step and the zwitterionic intermediate during the chain growth step. MMA and MMBL have a charge of around −0.018e on the C atom that is attacked by the LB, exhibiting intermediate reactivity. Finally, ES carries a significant negative charge on the β-carbon that then is less prone to react with the LB and the zwitterionic intermediate.

Overall, this DFT-based theoretical analysis indicates that substituents in the α and β positions of the monomer substantially modulate the monomer reactivity because they not only impact the steric congestion around the active center during the polymerization but also alter the electron density on the conjugated β-carbon in the M-MAD adduct.

Unique Materials Accessible by CSC-LPP. Equipped with a fundamental understanding of the complex CSC relationships and the resultant polymerization behavior of various mixtures of the monomer scope, we designed several materials uniquely accessible through this methodology, serving as templates for future materials innovations. Overall, these examples illustrate the potential of CSC-LPP to achieve advanced BCP microstructures in one pot and one step from mixed monomer feeds.

We postulated that ^{n}BA, ^{t}BA, and MMA could be a compatible triplet of comonomers that should sequence in that respective order based on the consecutive constructive k_p and K_{eq} relationships (Scheme 1). To test this hypothesis, we

Scheme 1. Synthesis of ABC Tri-BCP in One Pot and One Step

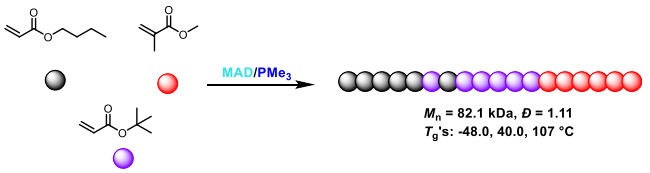

premixed ^{n}BA, ^{t}BA, MMA, and MAD in toluene at a 200:200:200:4 molar ratio with $[M]_0$ = 0.60 M. We then added 1 equivalent of PMe_3 (since this base usually produces better sequencing between ^{n}BA and ^{t}BA) and tracked the monomer decay over time (Figure 8). Indeed, the ^{n}BA polymerizes rapidly followed by the ^{t}BA, followed by the MMA. Interestingly, between the ^{t}BA and MMA crossover, we observed a small tapering phase where the ^{t}BA curve becomes non-linear due to the effect of an excess of MMA on the equilibrium. Additionally, the MMA is obviously locked out of the reaction until both the ^{n}BA and ^{t}BA concentrations approach depletion. Thus, the proof of concept that at least three monomers can be sequenced sufficiently in one pot/one step through CSC is supported. Three distinct T_g's were observed by DSC (Figure 8).

Next, we demonstrated one possible application of a destructively compounding k_p/K_{eq} scenario that can be made useful. If we consider the sequencing behavior of MA vs MMBL, which produces a random copolymer, and combine

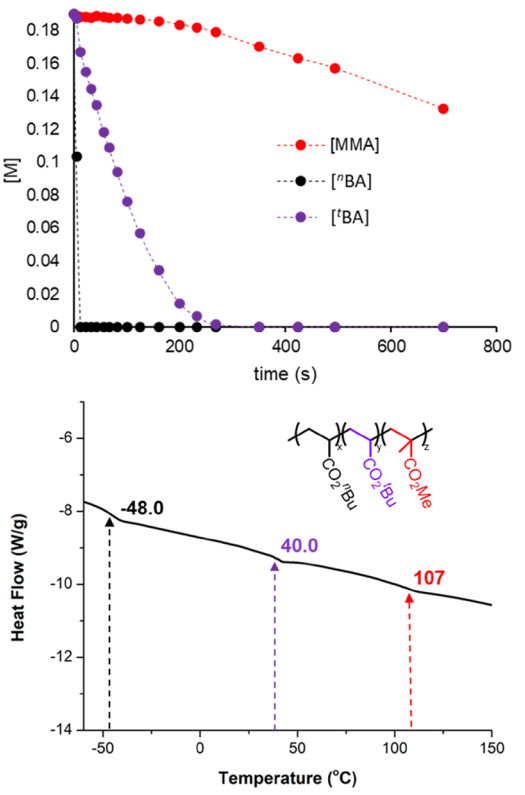

Figure 8. Monomer conversion over time (final point for MMA, 1400s, not shown) (top) and DSC trace (bottom) for ABC tri-BCP synthesized from a mixture of ^{n}BA, ^{t}BA, and MMA.

this pair with ^{t}BA, which results in a well sequenced diblock with MA and MMBL individually, we have a scenario in which the CSC of the triplet should yield a random PMA/PMMBL block followed by a homo-P^{t}BA block (Scheme 2). Since we

Scheme 2. Synthesis of Crosslinkable Diblock Terpolymers with Tunable T_g in One Pot and One Step

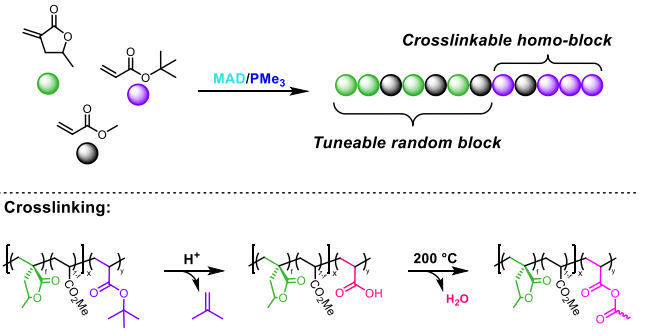

have shown that the P^{t}BA block can be thermolytically de-tert-butylized by temperatures exceeding 200 °C and such temperatures will not only promote de-tert-butylation but also the formation of anhydride crosslinks,[21,41−45] we can generate a material that contains a random phase consisting of two highly disparate monomers (PMA, T_g = −44.0 °C; PMMBL, T_g = 216 °C), wherein the T_g of this phase can be tuned by simple manipulation of the MMBL/MA feedstock ratio (see Table S1), while the size and mechanical contribution of the crosslinked phase can be tuned by the ^{t}BA feedstock ratio.

https://doi.org/10.1021/jacs.2c10568
J. Am. Chem. Soc. XXXX, XXX, XXX−XXX

We first examined this polymerization at an MMBL/MA/^{t}BA/MAD/PCy$_3$ ratio of 200:200:200:4:1, where $[M]_0$ = 1.80 M in DCM and tracked the monomer decay over time (Figure 9). As hypothesized, we observed rapid and

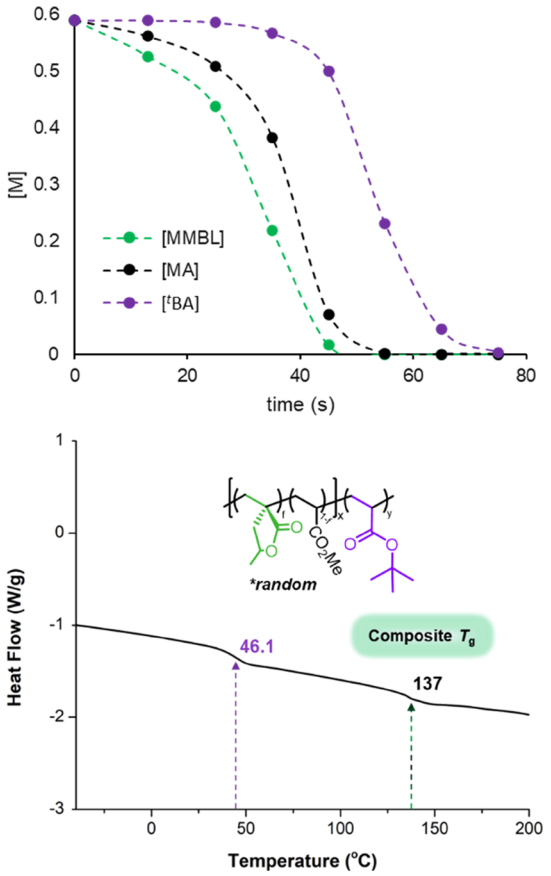

Figure 9. Monomer consumption over time (top) and DSC trace (bottom) for PMMBL-*ran*-PMA-*b*-P^{t}BA (200:200:200).

simultaneous incorporation of MMBL and MA, with a slight buildup of MA, before ^{t}BA was consumed. DSC analysis revealed one T_g very close to that of homo-P^{t}BA and one composite T_g, confirming a nearly perfect block of P^{t}BA and a random block of PMMBL/PMA. Varying the feed ratio of MMBL/MA indeed shifted this composite T_g accordingly, while the ^{t}BA T_g remained unchanged. Uniaxial tensile testing of the crosslinked terpolymer (300:1200:300, MMBL/MA/^{t}BA, M_n = 237 kDa, $Đ$ = 1.16 before crosslinking/processing) revealed material properties superior to any of the individual constituent homopolymers, with a Young's modulus of 2.23 ± 0.39 GPa, an ultimate strength of 38.3 ± 3.7 MPa, and elongation at break of 81 ± 24%. A representative stress–strain curve is shown in Figure 10.

Having satisfyingly demonstrated the ability of CSC to produce discrete AB and ABC BCPs from mixtures of two and three monomers, respectively, we further explored the possibility of forming an ABA triblock from a mixture of two monomers. If comonomers with suitable T_g's and mixing parameters are selected, such a microstructure has the potential to behave as a TPE,[46−48] resulting in a polymer with superior physical properties to thermoplastics.[49,50] TPE assembly typically requires a soft inner block capped by two hard outer blocks, corresponding to comonomers with disparate

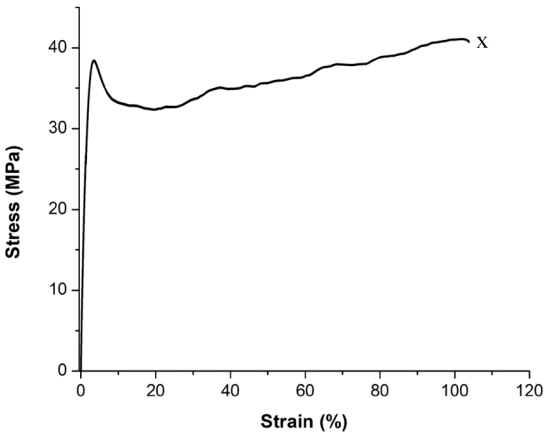

Figure 10. Tensile stress/strain profile (strain rate of 5 mm/min; 23 °C) of 300:1200:300 PMMBL-*ran*-PMA-*b*-P^{t}BA (crosslinked). Symbol "*x*" denotes the break point of the specimen.

thermal properties.[49] Fortunately, most of the soft monomers sequence before the hard monomers within our scope.

We previously reported a strategy employing CSC to produce ABA triblock copolymers in one pot and *two* steps[21] but have since devised a scheme by which this can be achieved in a true one-pot and *one*-step fashion through the use of a difunctional LB (Scheme 3). We began our analysis using ^{n}BA,

Scheme 3. LPP Using Mono- vs Difunctional LBs for the Preparation of Di- vs Tri-BCPs

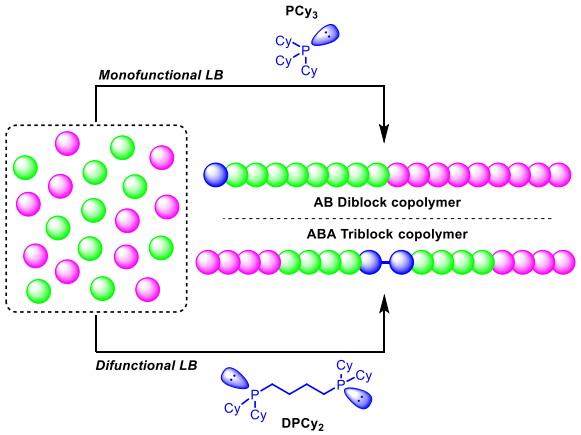

MMA, and the commercially available difunctional equivalent of PCy$_3$, μ^{butyl}(dicyclohexylphosphine)$_2$ (DPCy$_2$) (base **1**, Figure 11). As a 0.20 mL injection from a toluene stock solution, one equivalent of DPCy$_2$ was added to a solution of ^{n}BA, MMA, and MAD, premixed at a respective ratio of 1200:800:10 and $[M]_0$ = 1.0 M. As expected, the employment

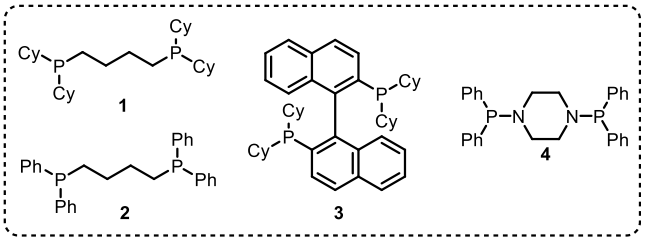

Figure 11. Di-initiating bisphosphine LBs screened for this study.

https://doi.org/10.1021/jacs.2c10568
J. Am. Chem. Soc. XXXX, XXX, XXX−XXX

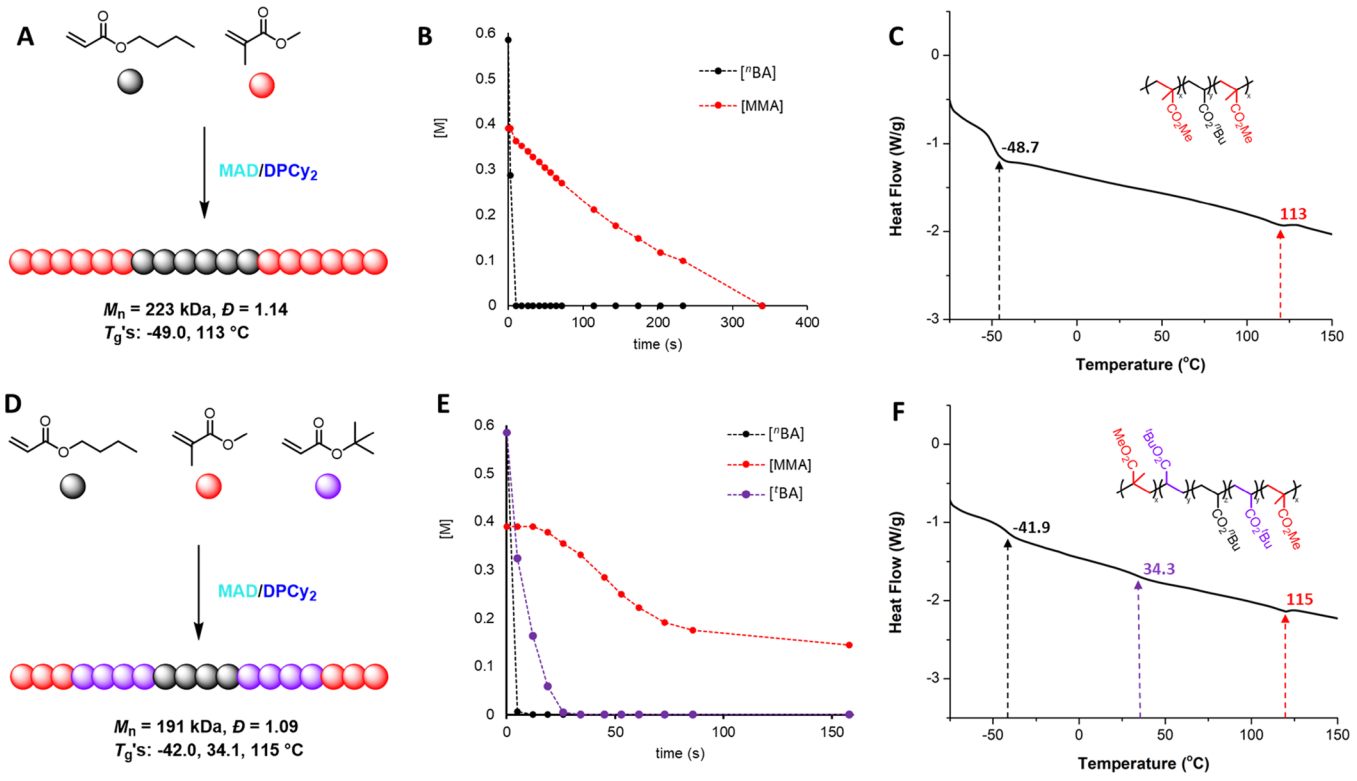

Figure 12. Schemes, kinetic profiles, and DSC traces for (A−C) triblock PMMA-*b*-P^{n}BA-*b*-PMMA and (D−F) pentablock PMMA-*b*-P^{t}BA-P^{n}BA-*b*-P^{t}BA-*b*-PMMA CSC (final point for MMA, 450 s, not shown).

of a di-initiator preserved the degree of comonomer sequence control; monomer conversion over time and DSC analysis supported the sequencing of ^{n}BA/MMA and the formation of PMMA-*b*-P^{n}BA-*b*-PMMA (Figure 12). Similarly, the CSC of ^{n}BA, ^{t}BA, and MMA using MAD/DPCy$_2$ produced the corresponding ABCBA pentablock PMMA-*b*-P^{t}BA-P^{n}BA-*b*-P^{t}BA-*b*-PMMA. Diphosphines with a bisaryl bridge (**3**) and bis-amino linkage (**4**) worked better, due to the enhanced stability of the phosphonium cation during propagation. Note that Zhang and co-workers previously applied this same strategy for the facile preparation of an ABA triblock using synthetically demanding pyridinylidenaminophosphine di-initiators.[51] Their report also verified that indeed both sides of the diphosphine initiated polymerization and acted as the true di-LB.

For imaging purposes, we replaced the soft P^{n}BA block with the double-bond containing, soft PAlA block in the synthesis of the well-defined ABA tri-BCP PMMA-*b*-PAIA-*b*-PMMA from a mixture of AlA and MMA (AlA/MMA/MAD/DPCy$_2$ = 500:500:10:1). Indeed, transmission electron microscopy (TEM) image of the tri-BCP showed clear microphase separation due to self-assembly of the tri-BCP (Figure 13). In contrast, the related di-BCP PMMA-*b*-PAIA prepared from a mixture of AlA and MMA (AlA/MMA/MAD/PCy$_2$ = 500:500:10:1) appeared largely featureless and revealed no such ordered, phase-separated morphology.

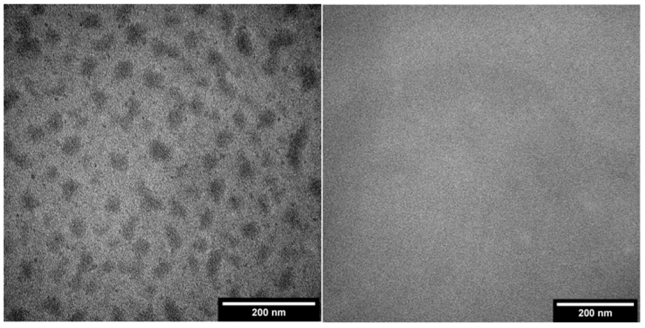

Figure 13. TEM images of tri-BCP PMMA-*b*-PAlA-*b*-PMMA produced by di-initiating LB DPCy$_2$ (left) and di-BCP PAlA-*b*-PMMA produced by mono-initiating LB PCy$_3$ (right).

CONCLUSIONS

We have demonstrated how LPP's unique polymerization mechanism, in which a monomer is preactivated by LA prior to entering the rate-determining propagation step, allows for the emergence of a biasing LA coordination equilibrium (K_{eq}) in the presence of multiple monomers with differing LA-affinities. Moreover, we showed how copolymer block resolution directly results from the relationship between this LA-activation bias and the inherently different rates of polymerization of each comonomer (k_p). Selecting representative monomers from a range of classes including acrylates, methacrylates, sorbates, acrylamides, and α-methylene lactones, we have quantified these CSC parameters for a suite of polar vinyl monomers and offered rationale for the observed trends, which were supported by computational modeling.

We showed that almost perfect block resolution is observed when both terms, K_{eq} and k_p, favor one comonomer and thus compound constructively; a copolymerization of monomers A and B results in a near perfect AB di-BCP when both $k_p^A > k_p^B$ and $K_{eq}^{A/B} > 1$. Through exploring the more nuanced examples in which these terms bias opposite monomers, we discovered a fascinating competition between kinetic and thermodynamic control over selective comonomer incorporation and resultant

https://doi.org/10.1021/jacs.2c10568
J. Am. Chem. Soc. XXXX, XXX, XXX−XXX

copolymer block resolution. When these parameters conflict with one another and therefore compound destructively, $k_p^A < k_p^B$ and $K_{eq}^{A/B} > 1$, random or tapered copolymer microstructure is generally observed. However, analyzing the extremes of these conflicting relationships revealed that both parameters were capable of overriding the other provided a sufficient difference in magnitude; a copolymerization of monomers A and B could still result in a near perfect AB diblock copolymer despite a conflicting CSC relationship if $k_p^A \ll k_p^B$, while $K_{eq}^{A/B} > 1$ or $k_p^A < k_p^B$, while $K_{eq}^{A/B} \gg 1$. This insight provides a fundamentally new understanding of the CSC mechanism and may be leveraged to control the sequence of previously considered incompatible monomer pairs.

This analysis of complex interplay between K_{eq} and k_p parameters was extended to the polymerization of mixtures of three monomers for the formation of triblock, pentablock, and unique random-diblock terpolymers, demonstrating how this methodology offers facile routes to unique copolymers with more advanced, sophisticated microstructures with potential material applications. Moreover, this work confirms the remaining unrealized potential of LPP, as the judicious selection of LA and LB enabled these discoveries. Therefore, incorporation of additional monomer classes, generation of innovative copolymers, and optimization of synthetic routes remain fruitful with further exploration of novel LPs.

■ ASSOCIATED CONTENT

Supporting Information

The Supporting Information is available free of charge at https://pubs.acs.org/doi/10.1021/jacs.2c10568.

Experimental and computational details and polymer synthesis and characterization data (PDF)

■ AUTHOR INFORMATION

Corresponding Authors

Laura Falivene − *Dipartimento di Chimica e Biologia, Università di Salerno, 84100 Fisciano, SA, Italy*; Email: lafalivene@unisa.it

Eugene Y.-X. Chen − *Department of Chemistry, Colorado State University, Fort Collins, Colorado 80523-1872, United States*; orcid.org/0000-0001-7512-3484; Email: eugene.chen@colostate.edu

Authors

Liam T. Reilly − *Department of Chemistry, Colorado State University, Fort Collins, Colorado 80523-1872, United States*; orcid.org/0000-0003-1469-7606

Michael L. McGraw − *Department of Chemistry, Colorado State University, Fort Collins, Colorado 80523-1872, United States*

Francesca D. Eckstrom − *Department of Chemistry, Colorado State University, Fort Collins, Colorado 80523-1872, United States*

Ryan W. Clarke − *Department of Chemistry, Colorado State University, Fort Collins, Colorado 80523-1872, United States*

Kevin A. Franklin − *Department of Chemistry, Colorado State University, Fort Collins, Colorado 80523-1872, United States*

Eswara Rao Chokkapu − *Department of Chemistry, Colorado State University, Fort Collins, Colorado 80523-1872, United States*

Luigi Cavallo − *Physical Sciences and Engineering Division, KAUST Catalysis Center, King Abdullah University of Science and Technology (KAUST), Thuwal 23955-6900, Saudi Arabia*; orcid.org/0000-0002-1398-338X

Complete contact information is available at: https://pubs.acs.org/10.1021/jacs.2c10568

Author Contributions

‖L.T.R. and M.L.M. contributed equally.

Notes

The authors declare no competing financial interest.

■ ACKNOWLEDGMENTS

We gratefully acknowledge support by the U.S. National Science Foundation (NSF-1904962). We also acknowledge Dr. Roy Geiss for his help in acquiring the TEM images.

■ REFERENCES

(1) Zhang, Y.; Miyake, G. M.; Chen, E. Y. X. Alane-Based Classical and Frustrated Lewis Pairs in Polymer Synthesis: Rapid Polymerization of MMA and Naturally Renewable Methylene Butyrolactones into High-Molecular-Weight Polymers. *Angew. Chem., Int. Ed.* **2010**, *49*, 10158−10162.

(2) Zhang, Y.; Miyake, G. M.; John, M. G.; Falivene, L.; Caporaso, L.; Cavallo, L.; Chen, E. Y. X. Lewis Pair Polymerization by Classical and Frustrated Lewis Pairs: Acid, Base and Monomer Scope and Polymerization Mechanism. *Dalton Trans.* **2012**, *41*, 9119−9134.

(3) Hong, M.; Chen, J.; Chen, E. Y. X. Polymerization of Polar Monomers Mediated by Main-Group Lewis Acid-Base Pairs. *Chem. Rev.* **2018**, *118*, 10551−10616.

(4) McGraw, M. L.; Chen, E. Y. X. Lewis Pair Polymerization: Perspective on a Ten-Year Journey. *Macromolecules* **2020**, *53*, 6102−6122.

(5) Wang, X.; Zhang, Y.; Hong, M. Controlled and Efficient Polymerization of Conjugated Polar Alkenes by Lewis Pairs Based on Sterically Hindered Aryloxide-Substituted Alkylaluminumitle. *Molecules* **2018**, *23*, 2564−2578.

(6) Takada, K.; Ito, T.; Kitano, K.; Tsuchida, S.; Takagi, Y.; Chen, Y.; Satoh, T.; Kakuchi, T. Synthesis of Homopolymers, Diblock Copolymers, and Multiblock Polymers by Organocatalyzed Group Transfer Polymerization of Various Acrylate Monomers. *Macromolecules* **2015**, *48*, 511−519.

(7) Wang, H.; Wang, Q.; He, J.; Zhang, Y. Living Polymerization of Acrylamides Catalysed by: N -Heterocyclic Olefin-Based Lewis Pairs. *Polym. Chem. J.* **2019**, *10*, 3597−3603.

(8) Chen, Y.; Shen, J.; Liu, S.; Zhao, J.; Wang, Y.; Zhang, G. High Efficiency Organic Lewis Pair Catalyst for Ring-Opening Polymerization of Epoxides with Chemoselectivity. *Macromolecules* **2018**, *51*, 8286−8297.

(9) Zhao, W.; Wang, Q.; He, J.; Zhang, Y. Chemoselective and Living/Controlled Polymerization of Polar Divinyl Monomers by N-Heterocyclic Olefin Based Classical and Frustrated Lewis Pairs. *Polym. Chem. J.* **2019**, *10*, 4328−4335.

(10) Gowda, R. R.; Chen, E. Y. X. Chemoselective Lewis Pair Polymerization of Renewable Multivinyl-Functionalized γ-Butyrolactones. *Philos. Trans. Royal Soc. A.* **2017**, *375*, No. 20170003.

(11) Zhang, P.; Zhou, H.; Lu, X. B. Living and Chemoselective (Co)Polymerization of Polar Divinyl Monomers Mediated by Bulky Lewis Pairs. *Macromolecules* **2019**, *52*, 4520−4525.

(12) McGraw, M. L.; Clarke, R. W.; Chen, E. Y. X. Compounded Sequence Control in Polymerization of One-Pot Mixtures of Highly Reactive Acrylates by Differentiating Lewis Pairs. *J. Am. Chem. Soc.* **2020**, *142*, 5969−5973.

(13) Bai, Y.; Wang, H.; He, J.; Zhang, Y. Rapid and Scalable Access to Sequence-Controlled DHDM Multiblock Copolymers by FLP Polymerization. *Angew. Chem., Int. Ed.* **2020**, *59*, 11613−11619.

(14) Hosoi, Y.; Takasu, A.; Matsuoka, S. I.; Hayashi, M. N-Heterocyclic Carbene Initiated Anionic Polymerization of (E,E)-

Methyl Sorbate and Subsequent Ring-Closing to Cyclic Poly(Alkyl Sorbate). *J. Am. Chem. Soc.* **2017**, *139*, 15005−15012.
(15) Zhang, Y.; Schmitt, M.; Falivene, L.; Caporaso, L.; Cavallo, L.; Chen, E. Y. X. Organocatalytic Conjugate-Addition Polymerization of Linear and Cyclic Acrylic Monomers by N-Heterocyclic Carbenes: Mechanisms of Chain Initiation, Propagation, and Termination. *J. Am. Chem. Soc.* **2013**, *135*, 17925−17942.
(16) Li, X.; Chen, C.; Wu, J. Lewis Pair Catalysts in the Polymerization of Lactide and Related Cyclic Esters. *Molecules* **2018**, *23*, 189−201.
(17) Li, X. Q.; Wang, B.; Ji, H. Y.; Li, Y. S. Insights into the Mechanism for Ring-Opening Polymerization of Lactide Catalyzed by $Zn(C_6F_5)_2$/Organic Superbase Lewis Pairs. *Catal. Sci. Technol.* **2016**, *6*, 7763−7772.
(18) Piedra-Arroni, E.; Ladavière, C.; Amgoune, A.; Bourissou, D. Ring-Opening Polymerization with $Zn(C_6F_5)_2$ -Based Lewis Pairs: Original and Efficient Approach to Cyclic Polyesters. *J. Am. Chem. Soc.* **2013**, *135*, 13306−13309.
(19) Li, C.; Zhao, W.; He, J.; Zhang, Y.; Zhang, W. Single-Step Expeditious Synthesis of Diblock Copolymers with Different Morphologies by Lewis Pair Polymerization-Induced Self-Assembly. *Angew. Chem., Int. Ed.* **2022**, *61*, No. e202202448.
(20) Sun, X. Y.; Ren, W. M.; Liu, S. J.; Jia, Y. B.; Wang, Y. M.; Lu, X. B. Tandem Lewis Pair Polymerization and Organocatalytic Ring-Opening Polymerization for Synthesizing Block and Brush Copolymers. *Molecules* **2018**, *23*, 468−474.
(21) Clarke, R. W.; McGraw, M. L.; Newell, B. S.; Chen, E. Y. X. Thermomechanical Activation Achieving Orthogonal Working/Healing Conditions of Nanostructured Tri-Block Copolymer Thermosets. *Cell Rep. Phys. Sci.* **2021**, *2*, No. 100483.
(22) McGraw, M. L.; Clarke, R. W.; Chen, E. Y. X. Synchronous Control of Chain Length/Sequence/Topology for Precision Synthesis of Cyclic Block Copolymers from Monomer Mixtures. *J. Am. Chem. Soc.* **2021**, *143*, 3318−3322.
(23) McGraw, M. L.; Reilly, L. T.; Clarke, R. W.; Cavallo, L.; Falivene, L.; Chen, E. Y. X. Mechanism of Spatial and Temporal Control in Precision Cyclic Vinyl Polymer Synthesis by Lewis Pair Polymerization. *Angew. Chem., Int. Ed.* **2022**, *61*, No. e202116303.
(24) Chen, E. Y. X. Coordination Polymerization of Polar Vinyl Monomers by Single-Site Metal Catalysts. *Chem. Rev.* **2009**, *109*, 5157−5214.
(25) Naumann, S. Synthesis, Properties & Applications of N-Heterocyclic Olefins in Catalysis. *Chem. Commun.* **2019**, *55*, 11658−11670.
(26) Kiesewetter, M. K.; Shin, E. J.; Hedrick, J. L.; Waymouth, R. M. Organocatalysis: Opportunities and Challenges for Polymer Synthesis. *Macromolecules* **2010**, *43*, 2093−2107.
(27) Flanigan, D. M.; Romanov-Michailidis, F.; White, N. A.; Rovis, T. Organocatalytic Reactions Enabled by N-Heterocyclic Carbenes. *Chem. Rev.* **2015**, *115*, 9307−9387.
(28) Fèvre, M.; Pinaud, J.; Gnanou, Y.; Vignolle, J.; Taton, D. N-Heterocyclic Carbenes (NHCs) as Organocatalysts and Structural Components in Metal-Free Polymer Synthesis. *Chem. Soc. Rev.* **2013**, *42*, 2142−2172.
(29) Schuldt, R.; Kästner, J.; Naumann, S. Proton Affinities of N-Heterocyclic Olefins and Their Implications for Organocatalyst Design. *J. Org. Chem.* **2019**, *84*, 2209−2218.
(30) MacMillan, D. W. C. The Advent and Development of Organocatalysis. *Nature* **2008**, *455*, 304−308.
(31) Naumann, S.; Dove, A. P. N-Heterocyclic Carbenes for Metal-Free Polymerization Catalysis: An Update. *Polym. Int.* **2015**, *65*, 16−27.
(32) Stephan, D. W.; Erker, G. Chemie Frustrierter Lewis-Paare: Entwicklung Und Perspektiven. *Angew. Chem. Int. Ed.* **2015**, *127*, 6498−6541.
(33) Stephan, D. W. Frustrated Lewis Pairs: From Concept to Catalysis. *Acc. Chem. Res.* **2015**, *48*, 306−316.
(34) Jupp, A. R.; Stephan, D. W. New Directions for Frustrated Lewis Pair Chemistry. *Trends Chem.* **2019**, *1*, 35−48.
(35) Stephan, D. W. The Broadening Reach of Frustrated Lewis Pair Chemistry. *Science* **2016**, *354*, 479−484.
(36) Knaus, M. G. M.; Giuman, M. M.; Pöthig, A.; Rieger, B. End of Frustration: Catalytic Precision Polymerization with Highly Interacting Lewis Pairs. *J. Am. Chem. Soc.* **2016**, *138*, 7776−7781.
(37) Gowda, R. R.; Chen, E. Y.-X. Methylene Butyrolactone Polymers. In *Encyclopedia of Polymer Science and Technology*, Mark, H. F., Ed., 4th ed; Wiley, Hoboken, 2014; Vol. *8*, pp 235−271.
(38) Agarwal, S.; Jin, Q.; Maji, A. Biobased Polymers from Plant-Derived Tulipalin A. *ACS Symp. Ser.* **2012**, *1105*, 197−212.
(39) Kitson, R. R. A.; Millemaggi, A.; Taylor, R. J. K. The Renaissance of α-Methylene-γ-butyrolactones: New Synthetic Approaches. *Angew. Chem., Int. Ed.* **2009**, *48*, 9426−9451.
(40) Falivene, L.; Cao, Z.; Petta, A.; Serra, L.; Poater, A.; Oliva, R.; Scarano, V.; Cavallo, L. Towards the Online Computer-Aided Design of Catalytic Pockets. *Nat. Chem.* **2019**, *11*, 872−879.
(41) Filippov, A. D.; van Hees, I. A.; Fokkink, R.; Voets, I. K.; Kamperman, M. Rapid and Quantitative De- Tert-Butylation for Poly(Acrylic Acid) Block Copolymers and Influence on Relaxation of Thermoassociated Transient Networks. *Macromolecules* **2018**, *51*, 8316−8323.
(42) Schaefgen, J. R.; Sarasohn, I. M. Observations on the Thermolytic Decomposition of Poly(Tert-Butyl Acrylate). *J. Polym. Sci.* **1962**, *58*, 1049−1061.
(43) Li, G. H.; Yang, P. P.; Gao, Z. S.; Zhu, Y. Q. Synthesis and Micellar Behavior of Poly(Acrylic Acid-b-Styrene) Block Copolymers. *Colloid Polym. Sci.* **2012**, *290*, 1825−1831.
(44) Qiao, Z.; Qiu, T.; Liu, W.; Guo, L.; Li, X. Novel Tri-Block Copolymers of Poly(Acrylic Acid)-: B -Poly(2,2,3,3,4,4,4-Hexafluorobutyl Acrylate)- b -Poly(Acrylic Acid) Prepared via Two-Step RAFT Emulsion Polymerization. *Polym. Chem.* **2016**, *7*, 3993−3997.
(45) Grant, D. H.; Grassie, N. The Thermal Decomposition Poly(t-Butyl Methacrylate). *Polymer* **1960**, *1*, 445−455.
(46) Spontak, R. J.; Pate, N. P. Thermoplastic Elastomers: Fundamentals and Applications. *Curr. Opin. Colloid. Interface Sci.* **2000**, *5*, 333−340.
(47) Espinosa, E.; Charleux, B.; D'Agosto, F.; Boisson, C.; Tripathy, R.; Faust, R.; Soulié-Ziakovic, C. Di- and Triblock Copolymers Based on Polyethylene and Polyisobutene Blocks Toward New Thermoplastic Elastomers. *Macromolecules* **2013**, *46*, 3417−3424.
(48) Holden, G. Thermoplastic Elastomers. In *Applied Plastics Engineering Handbook*, 1st ed.; Elsevier Inc., 2011, pp 77−91.
(49) Holden, G.; Bishop, E. T.; Legge, N. R. Thermoplastic Elastomers. In *Journal of Polymer Science, Part C: Polymer Symposia*; Wiley Subscription Services, Inc., A Wiley Company: New York, 1969; Vol. *26* (1), 37−57.
(50) Lambert-Diani, J.; Rey, C. New Phenomenological Behavior Laws for Rubbers and Thermoplastic Elastomers. *Eur. J. Mech. A. Solids.* **1999**, *18*, 1027−1043.
(51) Wan, Y.; He, J.; Zhang, Y.; Chen, E. Y. X. One-Step Synthesis of Lignin-Based Triblock Copolymers as High-Temperature and UV-Blocking Thermoplastic Elastomers. *Angew. Chem., Int. Ed.* **2022**, *61*, No. e202114946.

https://doi.org/10.1021/jacs.2c10568
J. Am. Chem. Soc. XXXX, XXX, XXX−XXX